JOURNAL OF Applied Polymer SCIENCE

Rheological and mechanical properties of cellulose/LDPE composites using sustainable and fully renewable compatibilisers

Philip Benjamin Vincent Scholten,[1,2] **Mürüvvet Begüm Özen**,[3] **Zafer Söyler**,[2] **Jean-Michel Thomassin**,[1] **Manfred Wilhelm**,[3] **Christophe Detrembleur**,[1] **Michael Alfred Robert Meier**[2,4]

[1]Department of Chemistry, Center for Education and Research on Macromolecules (CERM), CESAM Research Unit, University of Liege, Sart-Tilman B6a, Liege 4000, Belgium

[2]Materialwissenschaftliches Zentrum MZE, Karlsruhe Institute of Technology (KIT), Institute of Organic Chemistry (IOC), Straße am Forum 7, Karlsruhe 76131, Germany

[3]Chair for Polymer Materials, Karlsruhe Institute of Technology (KIT), Institute of Technical and Polymer Chemistry, Engesserstraße 18, Karlsruhe 76128, Germany

[4]Laboratory of Applied Chemistry, Institute of Toxicology and Genetics (ITG), Karlsruhe Institute of Technology (KIT), Hermann-von-Helmholtz-Platz 1, Eggenstein-Leopoldshafen 76344, Germany

Correspondence to: M. A. R. Meier (E-mail: m.a.r.meier@kit.edu)

ABSTRACT: Cellulose composites with polyethylene (PE) permit to reinforce this commodity polymer, while at the same time introducing renewable content and thus minimizing the use of petroleum-based feedstocks. Herein, we report on two fully renewably sourced and sustainably synthesized compatibilisers based on amylose and starch, which allow for such cellulose dispersion in low-density PE (LDPE). These compatibilisers advantageously combine the hydrophilicity of carbohydrates with the hydrophobicity of fatty acids. Upon extrusion of cellulose, LDPE, and the compatibilisers, a significantly improved dispersion of cellulose within LDPE was observed using rheology at loadings of 10 wt % cellulose and 5–15 wt % compatibiliser. Moreover, an improved interfacial adhesion was observed using scanning electron microscopy and was also confirmed by the mechanical properties, notably the Young's modulus, as a result of the good stress transfer between filler and matrix material. This study highlights the potential of fully renewable compatibilisers for the preparation of composites of cellulose and the commodity plastic LDPE. © 2019 The Authors. *Journal of Applied Polymer Science* published by Wiley Periodicals, Inc. J. Appl. Polym. Sci. **2019**, *137*, 48744.

KEYWORDS: blends; cellulose and other wood products; compatibilization; phase behavior; rheology

Received 11 July 2019; accepted 11 November 2019

DOI: 10.1002/app.48744

INTRODUCTION

Cellulose fibers are an extremely attractive reinforcing filler for composite materials, as they are biodegradable, nontoxic, and of extremely high strength.[1–4] The origin of cellulose and the type of its extraction from biomass play a key role in the determination of its final properties.[1,5–7] Especially crystalline nanocellulose (CNC) has been the focus of many studies in the past,[4,5,7,8] as CNCs have the highest strength possible for cellulose fibers as a result of their high crystallinity. However, the isolation of the crystals from the otherwise amorphous cellulosic material requires lengthy and expensive pretreatments,[1,2,4,8,9] which make CNCs a value-added chemical with a current price of around 50 €/kg.[2] Analogous to the classical paper manufacturing, these nanocrystals are present as a salt and an aqueous dispersion of these CNCs is necessary to obtain isolated fibers, rendering their incorporation into hydrophobic matrices very difficult.[10,11] Thus, the extrusion of CNCs is extremely challenging, as special equipment is necessary to remove the water during the process, still hampering its industrial implementation.[3,12] A different type of cellulose fiber is therefore needed for an industrially feasible large-scale production of cellulose composites and several other

Additional Supporting Information may be found in the online version of this article.

P. B. V. Scholten and B. M. Özen contributed equally to this article.

methods are being investigated.[2] A particularly promising example is bulk cellulose obtained as a side product from the production of lignin and other wood-derived high-value chemicals via different pulping methods.[13] For instance, the acetosolv process (extraction using water containing acetic acid) results in cellulose fibers with a typical width below 20 μm and several hundreds micrometer in length, which are slightly acetylated. This is in contrast to organsolv cellulose (extraction using ethanol or methanol), which mainly contains alcohol groups.[14] The acetosolv process is advantageous compared to organsolv processes in that no high pressure equipment is needed, benign and nontoxic solvents are used, and that the bleeching of the cellulose can be performed directly after the end of the extraction.[14] Available as a side or waste product from an environmentally friendly process, compared to classical paper and CNC production methods, such fibers are more sustainable than CNCs and are thus a promising candidate for the production of reinforced composite materials.

Commodity plastics reinforced with cellulose are one of the main applications of cellulose and have been a main target for many researchers over the last decades.[1–4,15–17] The main objective, particularly for polyolefins, for example, polyethylene (PE), is to increase the material's strength with the added advantage of increasing the renewable content of the material. The major challenge for such composites of hydrophilic cellulose and hydrophobic polyolefins is the lack of compatibility between the two. The poor interfacial adhesion within the composite leads to very poor dispersion of the cellulose fibers, which tend to aggregate, thus resulting in poor material properties. Different routes have been employed to defeat this problem, ranging from the use of grafting agents,[18–21] and reactive extrusion,[22,23] to the functionalisation of one or both components.[2,16,24–28] Among these, the use of compatibilisers or coupling agents is particularly attractive, as these often polymeric molecules can be precisely synthesized and tuned in a controlled manner, thus allowing the effects of the molecular structure on the dispersion of cellulose to be closely investigated and optimized.

Herein, we report on the use of new renewable compatibilisers for the preparation of cellulose-reinforced low-density PE (LDPE) composites. These compatibilisers are based on starch and amylose, branched structural analogues of cellulose [Scheme 1 (a)], which are transesterified using high oleic sunflower oil to attach fatty acid chains onto its hydroxy groups [Scheme 1(b)], as reported in a previous publication.[29] In this catalytic process, a processable polymeric material is obtained, combining the hydrophilicity of a glucose repeat unit along the main chain with the hydrophobicity of a fatty acid side chain. It is envisaged that these materials are able to interact with both cellulose and LDPE and allow for a compatibilisation of such cellulose/LDPE

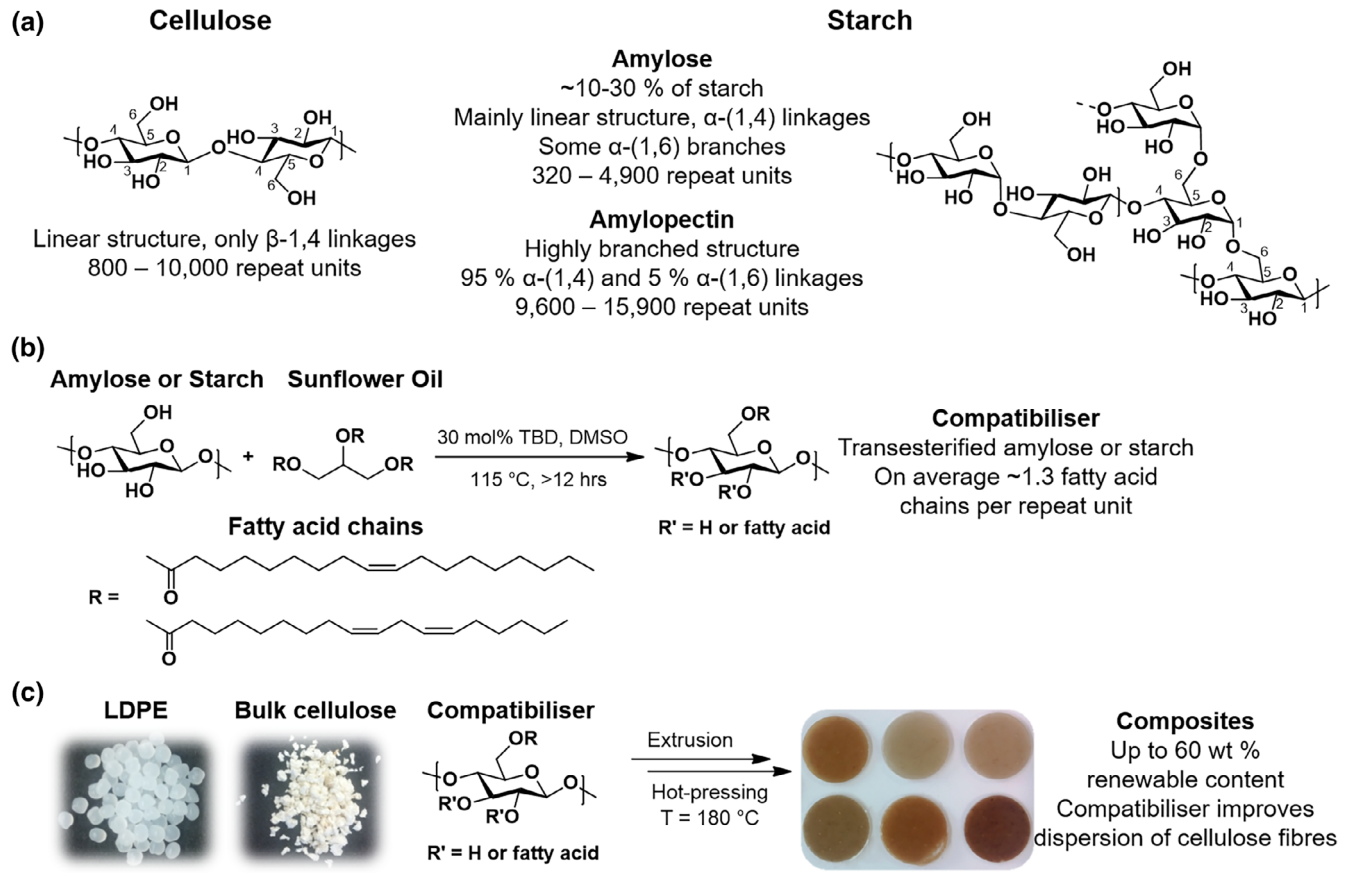

Scheme 1. (a) Structures of cellulose and starch with key parameters of their structure, (b) synthesis of amylose- or starch-based compatibiliser using high oleic sunflower oil,[29] and (c) the preparation of composites using LDPE, bulk cellulose, and the renewable compatibilisers prepared according to Meier *et al.*[29] [Color figure can be viewed at wileyonlinelibrary.com]

composites. Previous studies have shown that the acylation of cellulose with fatty acids[30] and the use of epoxidised plant oils as compatibilisers[22] are effective strategies to improve the material properties of PE. Furthermore, starch has been used as an additive in polyolefin matrices in the past.[31–33] The cellulose/LDPE composites investigated in this study were prepared using extrusion [Scheme 1(c)], which is industrially one of the most attractive methods of polyolefin processing. The efficacy of the compatibilisers was screened at a 10 wt % loading of cellulose using rheological analysis and microscopy, while the quest for composites containing up to 50 wt % renewable fraction was also investigated. Further insights into the dispersion of cellulose fibers within the composite and the material properties were obtained by scanning electron microscopy (SEM), stress–strain measurements, and thermal analyses.

EXPERIMENTAL SECTION

Materials

LDPE was kindly provided by INEOS Polymers & Olefins Europe and had the following characteristics: density: 920 kg/m^3; melt index MI2.16 (190 °C/2.16 kg; ISO 1133-1): 8.5 g/10 min; molecular weight: M_n = 17 300 g mol^{-1}, M_w = 126 000 g mol^{-1}; melting temperature (T_m): 107 °C; crystallinity: 44%. The crystallinity was calculated by using the enthalpy of melting measured by differential scanning calorimetry (DSC): Cryst = (ΔH_m measured/$\Delta H_{m\,\infty}$) × 100, where $\Delta H_{m\,\infty}$ = 293 J g^{-1}, the enthalpy of melting for 100% crystalline PE.[34]

The cellulose pulp was obtained by pulping European beech wood (*Fagus sylvatica L.*) using acetic acid followed by hydrogen peroxide (30%w/w in H_2O, Aldrich) bleaching. Cellulose characterization is provided in the Supporting Information (Figure S1–S2). The transesterified amylose or starch were prepared according to a recent publication by Meier *et al.*[29] using high oleic sunflower oil provided by Cargill (94.5% of acid chains were unsaturated, with 88.7% being monounsaturated, i.e., oleic acid, as determined by ^{1}H NMR) and maize starch purchased in a local supermarket. Cellulose, starch, and amylose (Aldrich) were dried at 100 °C in a vacuum oven overnight prior to use. 1,5,7-Triazabicyclo[4.4.0]dec-5-ene (98%, Aldrich) and dimethyl sulfoxide (anhydrous, > 99.9%, Aldrich) were used as received. These polymeric materials have been previously characterized in detail[29] and showed a glass transition temperature (T_g) at 90 °C while no T_m was observed prior to their decomposition from 270 °C onwards.

Preparation of Composites

The different composites were prepared according to Table I. The cellulose, modified amylose, and modified starch were cut into small pieces, premixed with a spatula and, along with LDPE, inserted into a Haake Mini 5 g twin-screw extruder at 180 °C and 30 rpm. Once the sample was inserted, the rpm was increased to 80. The pure LDPE was also extruded under the same conditions to have the same thermal and shear history as the composites samples. Subsequently, the samples were compression-molded under vacuum at 120 °C and 10 kN pressure for 10 min in a laboratory press to make 1.1 mm thick disks of 25 mm diameter. The cooled films were then analyzed by TGA, DSC, SEM, rheology, and stress–strain measurements.

Table I. Composition of the Composites in wt % of a Total of 5 g of Sample

Entry	Sample code	LDPE (wt %)	Cellulose (wt %)	Compatibiliser (mA, A, mS or S)
1	C0mA/mS0	100	0	0
2	C10mA/mS5	85	10	5
3	C10mA/mS10	80	10	10
4	C10mA/mS15	75	10	15
5	C0mA/mS10	90	0	10
6	C10mA/mS0	90	10	0
7	C10A/S10	80	10	10
8	C0A/S10	90	0	10
9	C45mA/mS10	45	45	10
10	C45mA/mS0	55	45	0

A, amylose; LDPE, low-density polyethylene; mA, modified amylose; mS, modified starch; S, starch.

Characterization

DSC was performed on a DSC Q100 instrument from TA Instruments by placing around 5 mg of sample in an aluminium pan. The sample was cooled to 0 °C, then heated to 140 °C, cooled to −90 °C, and heated to 200 °C at a heating/cooling rate of 10 °C/min. The last heating cycle was used for the determination of T_m.

Thermogravimetric analysis (TGA) was performed on a TGA Q500 instrument from TA Instruments. Around 10 mg of sample was heated to 600 °C at a rate of 20 °C/min.

The melt rheological properties of the samples were determined using an ARES G2 strain-controlled rotational rheometer from TA Instruments. All measurements were performed with 25 mm diameter parallel plate geometries under a nitrogen atmosphere. Dynamic strain sweep tests were performed at 150 °C with 1 rad/s for all the samples. Frequency dependence measurements were performed in the linear viscoelastic regime between 120 and 160 °C. The linear master curves of $G'(\omega)$ and $G''(\omega)$ at reference temperature T_{ref} = 150 °C were constructed via frequency dependency tests using the time–temperature-superposition (TTS) principle.[35] The TTS principle allows to increase the range of angular frequencies and thus gives more information about the sample.

SEM analysis was performed on an FEI Quanta 600 using a W gun using samples fractured in liquid nitrogen.

Stress–strain measurements were performed on an Instron 5594 tensile machine at a speed of 10 mm/min with a load capacity of 1000 N at room temperature. Young's modulus, tensile strength, and elongation at break were estimated by the average values of at least three composite samples.

RESULTS AND DISCUSSION

In this study, the effect of two different compatibilisers, starch and amylose transesterified with high oleic sunflower oil [modified amylose (mA) and modified starch (mS)], on the material properties of LDPE and cellulose (C; detailed analysis provided in Supporting Information) composites were investigated. As outlined in the introduction, cellulose was obtained from wood

chips, while LDPE was donated from an industrial partner and was produced via free-radical polymerization at elevated pressure and temperature. Each compatibiliser was first tested at different loadings for 10 wt % cellulose (entries 2–4 and 6, Table I) and then further at 45 wt % cellulose (entries 9 and 10, Table I). The obtained results were compared to reference samples (entries 1, 7, and 8, Table I) using nonmodified amylose (A) and nonmodified starch (S). For the sake of clarity, the amount of LDPE is omitted in the sample names, which reflect the respective sample composition (for instance, C0mA/mS0 for pure LDPE or C10mA/mS5 for a sample containing 85% LDPE, 10% cellulose and 5% starch-based compatibiliser, compare Table I).

Rheological Properties

The suitability of PE composite materials for various applications strongly depends on their processability.[36] Particularly the viscoelastic properties, amount of viscous (fluid-like) behavior quantitied by $G''(\omega_1)$ versus elastic (solid-like) behavior quantitied by $G'(\omega_1)$, and the thermal stability of the composites are important parameters and depend on the filler concentration and the extent of filler-matrix interaction. Rheology permits to measure these properties and allows to probe the microstructure of the composites, giving insights into the state of cellulose dispersion within the matrix.[28,37] The viscoelastic behavior can be investigated by measuring the storage modulus $G'(\omega_1, \gamma_0, T, t)$ (elastic contribution) and the loss modulus $G''(\omega_1, \gamma_0, T, t)$ (viscous contribution) during oscillatory shear measurements, in which the excitation frequency (ω_1), strain amplitude (γ_0), temperature (T), and time (t) are varied independently.[37] The linear viscoelastic region of the composites was determined by dynamic strain sweep measurements (Figure S3; Supporting Information), measuring $G'(\gamma)$ as a function of strain amplitude [γ_0 (t)] for all samples at 150 °C. The samples showed a linear viscoelastic region until γ_0=10%, except for the highest content of cellulose (C45mA/mS10), for which linear viscoelastic behaviors up to γ_0=4% were noted (Figure S3; Supporting Information). In the linear viscoelastic regime, G' is independent of applied strain and only depends on the microstructure at that temperature. Above this critical strain (γ), G' becomes dependent on the rate and magnitude of the applied strain and displays a more complex behavior.

Next, the samples were heated to 150 and 170 °C at an angular frequency of ω_1 = 1 rad/s for 1 h to determine their thermal stability in the linear viscoelastic regime (Figure S4–S5; Supporting Information). Samples exhibited a stable $G'(t)$ for both temperatures, indicative of the absence of degradation, except for samples with 45 wt % cellulose (C45mA10/S10 and C45mA0/S0). For all samples containing 45 wt % cellulose, a decrease in $G'(t)$ was observed over the 1 h period. This decrease was approximately 10% for C45mA10 and C45mS10, and above 15% for C45mA0/S0 at both temperatures (Figure S4–S5; Supporting Information). This phenomenon is not well understood, but possibly results from the loss of residual water in the cellulose fibers. Further investigations are needed to ascertain this hypothesis, for example, coupled TGA-IR measurements.

Once the thermal stability of the composites up to 170 °C was ensured for 10 wt % cellulose composites, the effect of the addition of cellulose and compatibiliser on the linear flow properties of the composites was studied by dynamic frequency sweep tests (Figure S6; Supporting Information), in which the storage modulus [$G'(\omega_1)$] is obtained as a function of angular frequency (ω_1) at reference temperature (T_{ref}) 150 °C using the TTS principle. In this kind of test, an increase of $G'(\omega_1)$ at low ω_1 is an indication of the dispersion of the filler within the matrix as the $G'(\omega_1)$ only depends on the microstructure of the composite at that temperature. Moreover, the appearance of a plateau signifies the breach of the percolation threshold. Above this threshold, the filler, in this case, cellulose fibers, forms an interconnected network through a space filling dispersion of the fibers within the matrix and improves the material properties through stress transfer from the matrix (low strength) to the filler (high strength).[36]

These tests showed that the addition of 10 wt % of cellulose to LDPE (C10mA0 and C10mS0) led to no enhancement of the storage modulus compared to LDPE (comparison of violet hexagons with black triangles, Figure S6; Supporting Information). Most likely the fibers formed agglomerates within the matrix and the addition of compatibiliser is needed to break these cellulose clusters and ensure their dispersion. The effect of the addition of 10 wt % of compatibiliser (without cellulose) on the rheological properties of the LDPE matrix was then investigated (Figure S6; Supporting Information). While the addition of modified or unmodified amylose to the LDPE matrix showed no significant changes in G' (filled pink pentagon and blue triangle, Figure S6; Supporting Information), slight changes for starch were observed. For modified starch, a 25% increase in G' at $\omega_1 \geq 10$ rad/s and a 90% G' increase at $\omega_1 \leq 1$ rad/s at 150 °C were observed, while for nonmodified starch, a 10% decrease in G' at $\omega_1 \geq 10$ rad/s and 60% increase in G' at $\omega_1 \leq 1$ rad/s at 150 °C were observed (hollow pink hexagon and blue triangle, Figure S6; Supporting Information). These differences in G' are very minor compared to the expected improvements once both cellulose and compatibiliser are added.

Next, the effect of the compatibiliser (5–15 wt %) in the presence of cellulose (10 wt %) was investigated using the same TTS principle at 150 °C. The storage modulus (G') increased successively with an increasing amount of compatibiliser (brown 5 wt %, blue 10 wt %, and green 15 wt %; Figure 1). At high frequencies ($\omega_1 > 10$ rad/s), G' was almost 200% higher for C10mA15 and 30% higher for C10mS15 compared to C0mA0. Furthermore, the appearance of a plateau of G' was noted at low frequencies ($\omega_1 < 10$ rad/s) for C10mA10, C10mA15 and C10mS15 (blue and green symbols in Figure 1). The plateau indicated a space filling dispersion of the cellulose fibers within the matrix. The otherwise agglomerated cellulose fibers formed an interconnected network within the matrix,[36] able to dissipate applied stresses much better within the material, increasing the storage modulus. The formation of such a network at this loading of cellulose is only possible for nonagglomerated cellulose fibers, that is, fibers which have an improved interfacial adhesion with the hydrophobic matrix. This is a direct reflection of the addition of the amphiphilic compatibilisers, which are able to provide interfacial interactions between the two materials.

It is worth highlighting that the plateau was significantly more pronounced for samples containing modified amylose (C10mA10 vs C10mS15), indicating a better compatibilising ability of the

modified amylose compared to its modified starch analogue. This can be further emphasized by comparing G' at ω_1 = 0.05 rad/s of samples C10mA15 and C10mS15, which was almost two times higher for amylose and constituted an 18-fold increase compared to pure LDPE. Another way of visualizing the improvement of the dispersion within the matrix is to plot the relative absolute complex viscosity ($|\eta^*|/|\eta^*|_0$) against the total filler and compatibiliser weight fraction (ϕ; Figure 2). The concentration necessary to have, for example, a factor 2 improvement in the complex viscosity (related to the dispersion of the cellulose fibers within the matrix) is reached between 15 and 20 wt % of filler and compatibiliser for amylose (i.e., C10mA5 and C10mA10), while it takes a higher amount to reach this value for starch, above 25 wt % (i.e., C10mS15; Figure 2). The behavior of the complex viscosity as a function of the weight fraction of compatibiliser and filler appears to be neatly described for amylose by the extended Einstein model, the modified Eilers,[38] Krieger–Dougherty,[39] or Mooney[40] models [see Table S1 (Supporting Information) for details] for suspensions of solids within a liquid while the modified Eilers model applies to the starch series. One possible explanation for the better performance of the modified amylose compatibiliser is that the linear structure of amylose [Scheme 1 (a)] was advantageous in the dispersion of cellulose in LDPE as it was able to enrobe the cellulose fibers more effectively, while starch, mainly composed of branched amylopectin [Scheme 1(a)], was not able to adhere to the fibers surface as effectively.

Moreover, increasing the amount of cellulose to 45 wt % without compatibiliser (C45mA/mS0) and with 10 wt % compatibiliser (C45mA/mS10) was investigated (Figure 3). Although a twofold increase in G' (ω_1) was obtained in the absence of compatibiliser, no plateau was observed for these samples (red symbols, Figure 3). Upon the addition of 10 wt % compatibiliser (C45mA/mS10), a 49-fold increase in G' for C45mA10 and a 38-fold increase in G' for C45mA10 were noted at ω_1 = 0.04 rad/s and a pronounced plateau at low frequencies was observed. These results confirmed that the addition of compatibiliser to the composite (C45mA/mS10) effectively improved the dispersion of the cellulose, compared to a simple mixture of LDPE and cellulose (C45mA/mS10), increasing the G' of the sample.

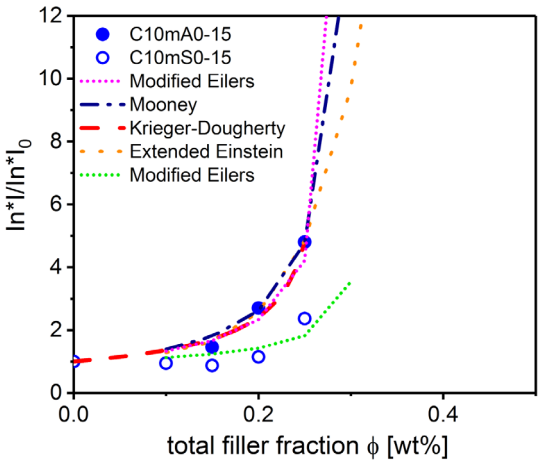

Figure 2. Relative absolute complex viscosity ($|\eta^*|/|\eta^*|_0$) as a function of the total filler (cellulose) and compatibiliser (mA or mS) fraction (ϕ, wt %) at angular frequency ω_1=0.05 rad/s for C0mA/mS0 and samples containing 10 wt % cellulose (C10mA0–15, C10mS0–15). Several models are fitted to the data points, which show an R-squared value above 0.97 [see 1 (Supporting Information) for further information]. [Color figure can be viewed at wileyonlinelibrary.com]

Scanning Electron Microscopy

To further improve the understanding of the dispersion of the cellulose fibers within the LDPE matrix, SEM images were taken. A difference in the cellulose dispersion can be seen when comparing samples with 45 wt % cellulose with and without compatibiliser (C45mA/mS10 vs C45mA/mS0). In the absence of compatibiliser, pull-out phenomena and large voids were observed between the fiber and the matrix [Figure 4(c)]. Samples with compatibiliser (C45mA/mS10) on the other hand showed enrobed cellulose fibers as well as a better adhesion of the polymer matrix with the cellulose fibers [Figure 4 (d,e)]. This indicated that the modified amylose and modified starch successfully increased the adhesion of the cellulose fibers within the matrix, which allowed for an improved dispersion of the cellulose fibers within the LDPE matrix, as observed by rheology. Unfortunately, no net difference could

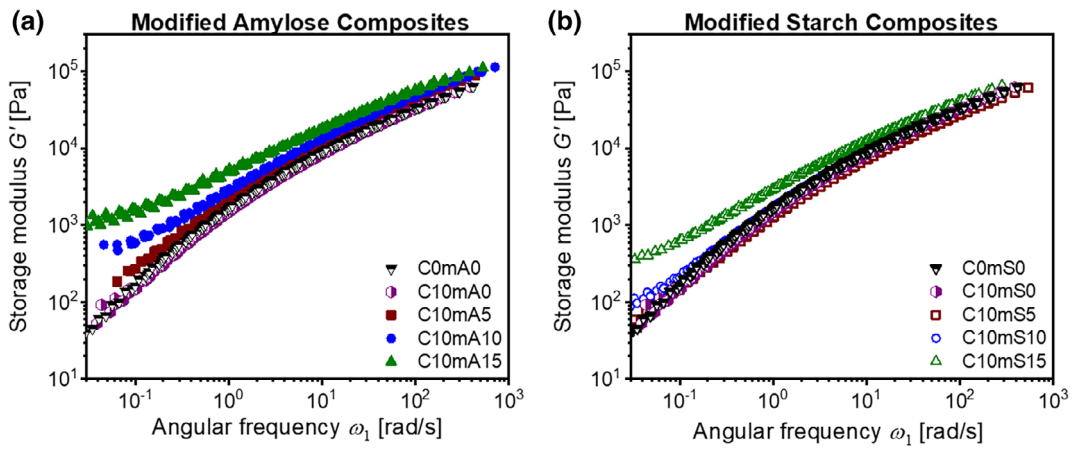

Figure 1. Storage modulus G' (ω_1) as a function of angular frequency ω_1 at T_{ref} = 150 °C as obtained via TTS for pure LDPE and for composites containing 10 wt % cellulose (C) with 5–15 wt % of (a) modified amylose (mA) and (b) modified starch (mS). [Color figure can be viewed at wileyonlinelibrary.com]

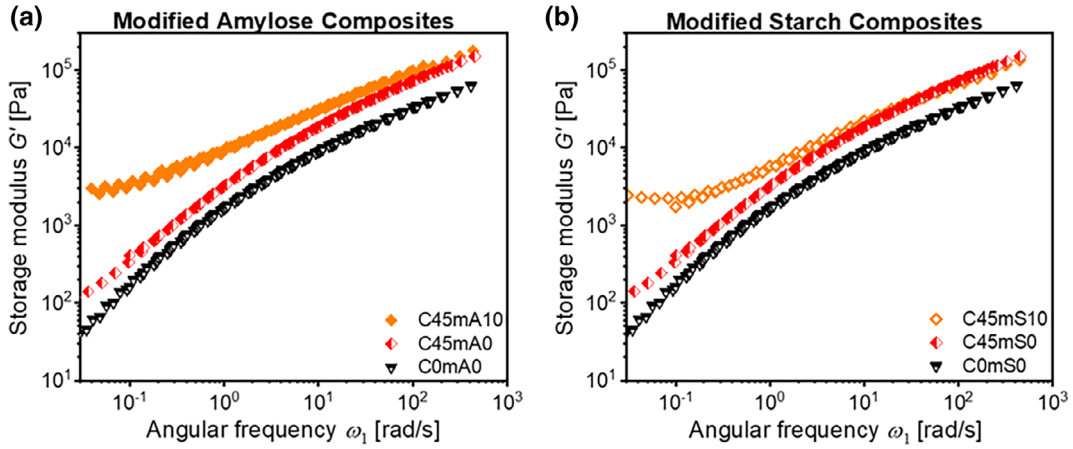

Figure 3. Storage modulus $G'(\omega_1)$ as a function of angular frequency ω_1 at T_{ref} = 150 °C as obtained via TTS for pure LDPE and for composites containing 45 wt % cellulose (C) and 10 wt % of (a) modified amylose (mA) and (b) modified starch (mS). [Color figure can be viewed at wileyonlinelibrary.com]

be observed in images for samples containing less cellulose, as no distinction between fibers, matrix, and compatibiliser could be made. Further investigations using transmission electron microscopy (TEM) also did not lead to a clarification because of the semicrystalline nature of the matrix, which gave rise to fuzzy regions in TEM pictures and the different components could again not be clearly distinguished.

Thermal Properties

The TGA analysis revealed a reduced thermal stability of the composite samples compared to pure LDPE and that their decomposition occurred in two steps. First, from 300 °C onwards, the cellulose and compatibiliser decomposed, followed by LDPE above 450 °C (Figure 5). The weight loss of the sample corresponds to the composition of the sample, for example, the weight of the sample C10mA/mS5 decreased by 15 wt % up until 400 °C, which corresponds to the content in cellulose (10 wt %) and compatibiliser (5 wt %) (see inset in Figure 5). An overall decrease in thermal stability was expected due to the lower thermal stability of cellulose. These values are in agreement with previously reported LDPE/starch blends.[32,33] In the DSC curves, no change in T_m compared to extruded LDPE was observed, apart from the effect of dilution in the enthalpy of melting (ΔH_m) (Figure S7; Supporting Information).

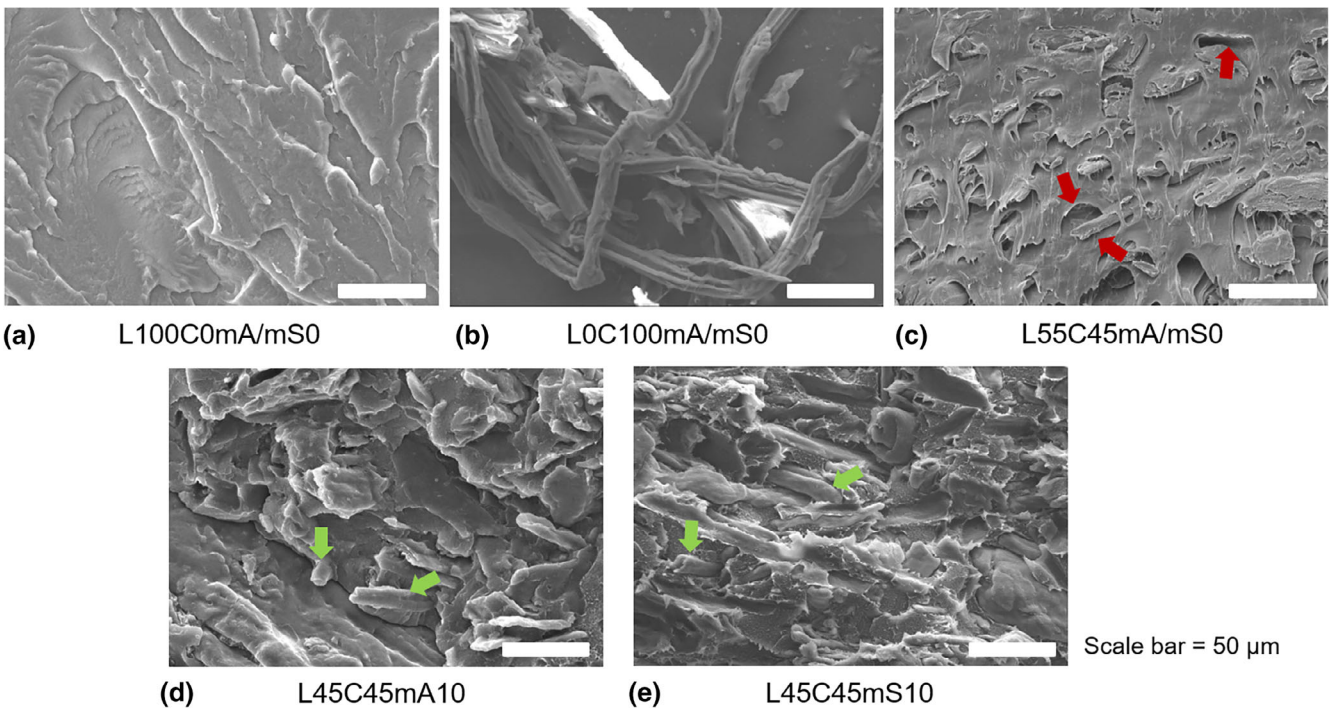

Figure 4. Scanning electron microscopy images of (a) pure LDPE (C0mA/mS0), (b) pure cellulose (C100mA/mS0), (c) composite C45mA/mS0, (d) composite C45mA10, and (e) composite C45mS10. Red arrows indicate pull-out phenomena and large voids; green arrows indicate enrobed fibers. [Color figure can be viewed at wileyonlinelibrary.com]

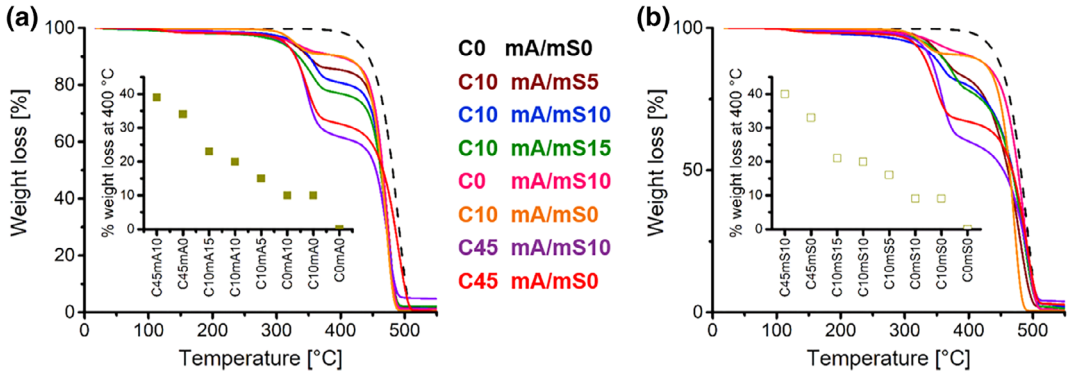

Figure 5. Thermogravimetric analysis curves of composites using (a) modified amylose and (b) modified starch compatibilisers and their respective reference samples with the inset showing the % weight loss at the first plateau at 400 °C. [Color figure can be viewed at wileyonlinelibrary.com]

Mechanical Properties

Once the successful dispersion of the cellulose fibers was demonstrated, the mechanical properties of the composites in the solid state were investigated by elongation stress–strain measurements (Table S2; Supporting Information). The main interest in adding cellulose fibers to a polymer matrix is to increase its Young's modulus and thus increase its strength. First, the effect of the compatibiliser on the Young's modulus of LDPE was investigated, which showed a negative effect on the Young's moduli, decreasing their value from 166 MPa (C0mA/mS0) to 123 and 112 MPa for modified amylose (C0mA10) and modified starch (C0mS10), respectively [entries 1, 5, and 12, Table S2 (Supporting Information); Figure 6]. This observation is similar to a previous report on the addition of vegetable oils to HDPE.22 A similar trend was observed for the addition of nonmodified amylose (C0A10) and starch (C0S10), showing decreased Young's moduli of 91 and 92 MPa, respectively, relative to the LDPE matrix (Table S2; Supporting Information). The addition of cellulose to the matrix without compatibiliser slightly increased the Young's modulus to 218 MPa (entries 6 and 13, Table S2; Supporting Information), corresponding to an increase of 31% relative to pure LDPE (166 MPa, entry 1, Table S2; Supporting Information).

Interestingly, in the presence of both cellulose and modified amylose (C10mA5–15, Figure 6) the relative increase of the Young's modulus is much larger. The largest relative increase (112%) was observed for the composite containing 10 wt % of modified amylose (261 vs 123 MPa, C10mA10 vs C0mA10, entries 3 and 5, Table S2; Supporting Information). Even though the rheological analyses showed that the cellulose was dispersed to an even better extent at 15 wt % compatibiliser loading (C10mA15), the Young's modulus dropped (202 MPa, entry 4, Table S2; Supporting Information) as a result of the softening effect of the compatibiliser. Nonetheless, the Young's modulus was still improved for C10mA15 compared to pure LDPE and a careful balance between the degree of cellulose dispersion and the Young's modulus needs to be found related to the type of application targeted.

Compared to the composites containing modified amylose, the addition of modified starch had a less significant impact on the Young's moduli. A maximum relative increase of 78% was observed for 5 wt % compatibiliser (C10mS5) and the addition of more compatibiliser led to a decrease to 140 MPa (C10mS15). This softening effect of the compatibiliser on the matrix material was more pronounced compared to modified amylose. Overall, these results support the rheological findings, which demonstrated that modified amylose led to a better cellulose dispersion compared to its starch analogues. It should be noted that, while the Young's modulus for samples containing cellulose and nonmodified amylose (C10A10) or nonmodified starch (C10S10)

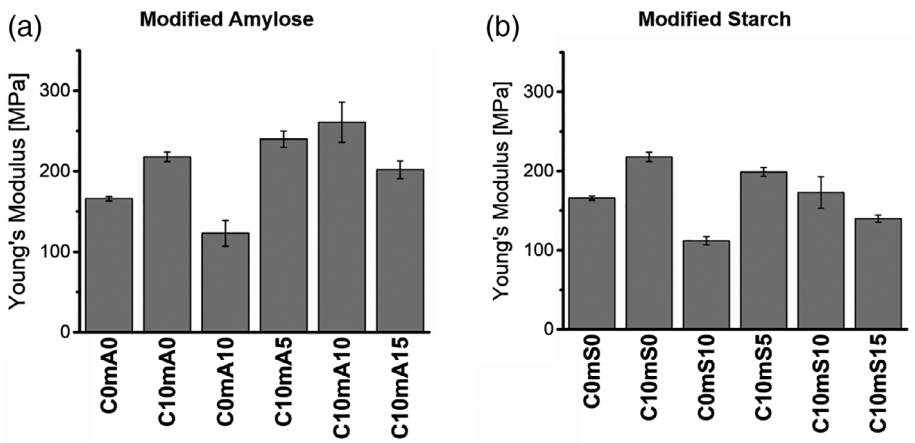

Figure 6. Young's moduli for composites with (a) modified amylose and (b) modified starch as compatibiliser and their respective reference samples.

were in the same range as the composites containing modified amylose (C10mA10) or modified starch (C10mS10), 261 versus 287 MPa for amylose and 237 versus 173 MPa for starch, the rheological analyses above clearly highlighted the absence of any cellulose dispersion within the matrix in the presence of non-modified amylose or nonmodified starch (Table S2; Supporting Information). This is directly reflected in the large standard deviation of the Young's modulus values (13–35%, Table S2; Supporting Information), as these composites are very inhomogeneous materials.

In all samples, a severe impact of the addition of cellulose on the elongation at break was observed, as values decreased from 185 to below 60% (Supporting Information). This is not unexpected, as a strengthening of the material (i.e., an increase in the Young's modulus) often triggers a decrease in its plastic elasticity leading to a more brittle material.

CONCLUSION

The preparation of LDPE composites using bulk cellulose fibers was shown to be possible using plant-oil and starch-based compatibilisers synthesized in a sustainable fashion. A clear improvement in the cellulose dispersion within the polymer matrix was observed using rheology and could be confirmed by SEM. Modified amylose showed a higher capacity to compatibilise cellulose within the LDPE matrix as a plateau in the storage modulus was observed at both 10 and 15 wt % compatibiliser loading with 10 wt % cellulose (C10mA10–15). This was also reflected by a relative increase of 112% (C10mA10) in terms of the Young's modulus. Modified starch, on the other hand, gave rise to a poorer dispersion of the cellulose and as a result, the composites' mechanical properties were not improved significantly, a relative increase of only 78% in the Young's modulus for C10mS5. This study highlights the promise of renewable compatibilisers for the preparation of reinforced polyolefin matrices using bulk cellulose fillers.

ACKNOWLEDGMENTS

The authors thank INEOS Polymers & Olefins Europe for providing LDPE. P.B.V.S., M.A.R.M., and C.D. thank the European Community in the frame of the ITN-Marie Curie Program "EJD-FunMat" (Grant number 641640). C.D. is a research director financed by the F.R.S.-FNRS. B.M.Ö. thanks the Ministry of National Education of the Republic of Turkey for financial support. The authors thank the Centre for Applied Research in Microscopy (CAREM) for the use of their SEM microscopes.

REFERENCES

1. Miao, C.; Hamad, W. Y. *Cellulose*. **2013**, *20*, 2221.
2. Abdul Khalil, H. P. S.; Bhat, A. H.; Ireana Yusra, A. F. *Carbohydr. Polym.* **2012**, *87*, 963.
3. Dufresne, A. *Curr. Opin. Colloid Interface Sci.* **2017**, *29*, 1.
4. Kontturi, E.; Laaksonen, P.; Linder, M. B.; Nonappa; Gröschel, A. H.; Rojas, O. J.; Ikkala, O. *Adv. Mater.* **2018**, *30*, 1703779.
5. Rajinipriya, M.; Nagalakshmaiah, M.; Robert, M.; Elkoun, S. *ACS Sustain. Chem. Eng.* **2018**, *6*, 2807.
6. Prakash Menon, M.; Selvakumar, R.; Suresh Kumar, P.; Ramakrishna, S. *RSC Adv.* **2017**, *7*, 42750.
7. Jonoobi, M.; Oladi, R.; Davoudpour, Y.; Oksman, K.; Dufresne, A.; Hamzeh, Y.; Davoodi, R. *Cellulose*. **2015**, *22*, 935.
8. Lee, K. Y.; Aitomäki, Y.; Berglund, L. A.; Oksman, K.; Bismarck, A. *Compos. Sci. Technol.* **2014**, *105*, 15.
9. Azouz, K. B.; Ramires, E. C.; Van Den Fonteyne, W.; El Kissi, N.; Dufresne, A. *ACS Macro Lett.* **2012**, *1*, 236.
10. Khoshkava, V.; Kamal, M. R. *Powder Technol.* **2014**, *261*, 288.
11. Peng, Y.; Sudhakaran Nair, S.; Chen, H.; Yan, N.; Cao, J. *ACS Sustain. Chem. Eng.* **2018**, *6*, 11078.
12. Oksman, K.; Mathew, A. P.; Bondeson, D.; Kvien, I. *Compos. Sci. Technol.* **2006**, *66*, 2776.
13. Tribot, A.; Amer, G.; Abdou Alio, M.; de Baynast, H.; Delattre, C.; Pons, A.; Mathias, J.-D.; Callois, J.-M.; Vial, C.; Michaud, P.; Dussap, C.-G. *Eur. Polym. J.* **2019**, *112*, 228.
14. Nimz, H. H.; Casten, R. *Holz als Roh- und Werkst.* **1986**, *44*, 207.
15. Eichhorn, S. J.; Dufresne, A.; Aranguren, M.; Marcovich, N. E.; Capadona, J. R.; Rowan, S. J.; Weder, C.; Thielemans, W.; Roman, M.; Renneckar, S.; Gindl, W.; Veigel, S.; Keckes, J.; Yano, H.; Abe, K.; Nogi, M.; Nakagaito, A. N.; Mangalam, A.; Simonsen, J.; Benight, A. S.; Bismarck, A.; Berglund, L. A.; Peijs, T. *J. Mater. Sci.* **2010**, *45*(1), 1.
16. Faruk, O.; Bledzki, A. K.; Fink, H. P.; Sain, M. *Prog. Polym. Sci.* **2012**, *37*, 1552.
17. Oksman, K.; Aitomäki, Y.; Mathew, A. P.; Siqueira, G.; Zhou, Q.; Butylina, S.; Tanpichai, S.; Zhou, X.; Hooshmand, S. *Compos. Part A Appl. Sci. Manuf.* **2016**, *83*, 2.
18. Yano, H.; Omura, H.; Honma, Y.; Okumura, H.; Sano, H.; Nakatsubo, F. *Cellulose*. **2018**, *25*, 3351.
19. Sakakibara, K.; Moriki, Y.; Yano, H.; Tsujii, Y. *ACS Appl. Mater. Interfaces*. **2017**, *9*, 44079.
20. Kaynak, B.; Spoerk, M.; Shirole, A.; Ziegler, W.; Sapkota, J. *Macromol. Mater. Eng.* **2018**, *303*, 1.
21. Wohlhauser, S.; Delepierre, G.; Labet, M.; Morandi, G.; Thielemans, W.; Weder, C.; Zoppe, J. O. *Macromolecules*. **2018**, *51*, 6157.
22. Oliveira De Castro, D.; Frollini, E.; Ruvolo-Filho, A.; Dufresne, A. *J. Polym. Sci. Part B Polym. Phys.* **2015**, *53*, 1010.
23. Pracella, M.; Haque, M. M. U.; Alvarez, V. *Polymers (Basel)*. **2010**, *2*, 554.
24. Singh, A. A.; Palsule, S. *J. Compos. Mater.* **2014**, *48*, 3673.
25. Prasad, N.; Agarwal, V. K.; Sinha, S. *Iran. Polym. J.* **2016**, *25*, 229.
26. Alidadi-Shamsabadi, M.; Behzad, T.; Bagheri, R.; Nari-Nasrabadi, B. *Polym. Compos.* **2015**, *36*, 2309.
27. Li, X.; Tabil, L. G.; Panigrahi, S. *J. Polym. Environ.* **2007**, *15*, 25.

28. Sdrobi, A.; Darie, R. N.; Totolin, M.; Cazacu, G.; Vasile, C. *Compos. Part B Eng.* **2012**, *43*, 1873.
29. Söyler, Z.; Meier, M. A. R. *ChemSusChem*. **2016**, *10*, 182.
30. Freire, C. S. R.; Silvestre, A. J. D.; Neto, C. P.; Gandini, A.; Martin, L.; Mondragon, I. *Compos. Sci. Technol.* **2008**, *68*, 3358.
31. Prinos, J.; Bikiaris, D.; Theologidis, S.; Panayiotou, C. *Polym. Eng. Sci.* **1998**, *38*, 954.
32. Tanrattanakul, V.; Panwiriyarat, W. *J. Appl. Polym. Sci.* **2009**, *114*, 742.
33. Sailaja, R. R. N. *Polym. Int.* **2005**, *54*, 286.
34. Wunderlich, B. The basis of thermal analysis. In Thermal Analysis, Elsevier Ltd: San Diego, California, **1990**.
35. Williams, M. L.; Landel, R. F.; Ferry, J. D. *J. Am. Chem. Soc.* **1955**, *77*, 3701.
36. Kontopoulou, M. In Applied Polymer Rheology: Polymeric Fluids with Industrial Applications; Kontopoulou, M., Ed., John Wiley & Sons, Inc.: Hoboken, New Jersey, **2012**.
37. Goodwin, J. W.; Hughes, R. W. Rheology for Chemists: An Introduction; The Royal Society of Chemistry: Cambridge, UK, **2000**.
38. Cwalina, C. D.; Harrison, K. J.; Wagner, N. J. *Soft Matter*. **2016**, *12*, 4654.
39. Krieger, I. M.; Dougherty, T. J. *Trans. Soc. Rheol.* **1959**, *3*, 137.
40. Mooney, M. *J. Colloid Sci.* **1951**, *6*, 162.